The influence of simulated missile warhead fragment damage on the aerodynamic characteristics of two-dimensional wings

A. J. Irwin
BAE Systems
Warton, UK

P. M. Render
P.M.Render@lboro.ac.uk
Department of Aeronautical and Automotive Engineering
Loughborough University
Loughborough, UK

ABSTRACT

The paper describes a method of representing damage on a wing due to multiple warhead fragments, and investigates two of the key variables: fragment impact density and hole diameter. The aerodynamic effects of the damage were quantified by wind-tunnel tests on a two-dimensional wing at a Reynolds number of 5×10^5. The wing was of hollow construction with leading and trailing-edge spars. In all of the cases tested, simulated fragment damage resulted in significant lift losses, drag increases and pitching moment changes. Increasing fragment density or hole size resulted in greater effects. To a first order approximation, both lift and drag increments at a given incidence were related to the percentage wing area removed. Surface flow visualisation showed that low fragment densities and small damage sizes resulted in a complex flow structure on the surface of the wing. This was made up of boundary-layer growth between the damage holes, attached wakes from the forward damage holes and separated surface flow over the rear of the wing. For these cases, individual hole patterns showed similar flow mechanisms

Paper No. 3875. Manuscript received 11 July 2012, revised version received 20 December 2012, accepted 7 February 2013.
https://doi.org/10.1017/S0001924000008472 Published online by Cambridge University Press

to those seen for larger scale gunfire damage cases. Increased fragment density and hole size resulted in upper surface flow separation at the first row of holes. Behind this separation, the flow was attached and consisted of the combined wakes from the forward damage holes. Investigations into the influence of internal model structure indicated that trends in coefficient changes were similar for both hollow and solid wings. However, the magnitudes of the effects were found to be smaller for hollow wings than for solid wings.

NOMENCLATURE

a	distance between damage hole centres
c	chord
C_d	drag coefficient
C_l	lift coefficient
C_m	pitching moment coefficient
C_p	pressure coefficient
$\mathrm{d}C_d$	change in drag coefficient due to damage
$\mathrm{d}C_l$	change in lift coefficient due to damage
$\mathrm{d}C_m$	change in pitching moment coefficient due to damage
x	co-ordinate along the wing chord
α	incidence
θ	rotation of damage grid
ρ_f	fragment density (average number of impacts per square metre)

Subscripts

Damaged	wing with damage from multiple missile warhead fragments
Undamaged	undamaged wing

1.0 INTRODUCTION

Survivability of an aircraft is dependent upon its vulnerability to damage caused by a variety of threat types, ranging from small arms, through to anti-aircraft artillery and missiles. During an aircraft's design stage, survivability enhancement techniques are implemented. These include assessments of the aircraft's capability to survive defined levels of battle damage. Generally, vulnerability assessments have tended to concentrate on structural integrity (e.g. equipment hardening, shielding, etc.), while paying only secondary attention to the possible aerodynamic effects of damage. This level of attention to aerodynamic factors may, in part, be attributed to the unavailability of relevant data. Combat damage which results in the physical removal of a portion of a wing or primary flight control surface, will undoubtedly lead to a reduction in aerodynamic performance and control degradation. This may lead to a reduction in mission effectiveness, and also to the possibility that the degradation in flight capability will be so severe that the chances of a successful return to base will be significantly reduced.

In their 2000 paper, Irwin and Render[1] indicated that few studies into the aerodynamic effects of damage to wings had been published before this date, and that generally these publications failed to explain the aerodynamic mechanisms. Irwin and Render then went on to describe wind tunnel tests on simulated gunfire damage on a two dimensional wing. The influence on force and moment coefficients was attributed to flow through the damage. This through flow was driven by

https://doi.org/10.1017/S0001924000008472 Published online by Cambridge University Press

the pressure differential between the upper and lower wing surfaces, and took one of two forms. The first form was a 'weak-jet' which formed an attached wake and resulted in small changes to force and moment coefficients. The second form resulted from either increased incidence, or damage size. This was the 'strong-jet', where through flow penetrated into the freestream flow, resulting in separation of the oncoming surface flow, and the development of a large separated wake with reverse flow. The effect on force and moment coefficients was significant. The findings of further battle damage studies have been published[2-4] but all of these papers have continued to study simulated gunfire damage. Gunfire damage is inflicted when one or more projectiles (artillery shell, small arms bullet, etc.) passes through the airframe to leave well defined, relatively large holes which are usually well separated and approximately round in shape. Frequently battle damage comprises of multiple holes in close proximity to each other. An example of such damage is from missile warheads which are designed to explode in close proximity to an aircraft and cause a predefined distribution of small high velocity fragments. The airframe is penetrated by some of the fragments to leave a large number of relatively small holes in close proximity to each other, typically in a roughly regular pattern. No aerodynamic investigations into the effects of damage due to missile warhead fragments have been previously published.

This paper introduces a method of representing damage on a two-dimensional wing from multiple fragments and outlines the key basic assumptions used in modelling. The results of the qualitative and quantitative investigations into the aerodynamic characteristics of the damaged wing are then presented.

2.0 DAMAGE MODELLING

There are potentially a vast range of damage cases that could be considered. To achieve a reasonable number of test cases, damage was assumed to arise from a representative single missile engagement. The geometry of missile engagements on target aircraft may still vary significantly, due to a large number of factors such as warhead design, missile approach geometry and relative velocities. However, the resulting damage remains broadly similar in most cases. Typically the warhead detonation may be anywhere between zero and many metres away from the aircraft, and the extent of damage over the aircraft structure may vary extensively. In the majority of cases, large portions of the wing and fuselage may sustain distributed fragmentation damage. Following detonation of the high-explosive charge, the warhead casing bursts in a predefined manner. As the casing breaks-up, a large number of similarly sized inert fragments are propelled outwards from the missile's longitudinal axes. This generates an expanding cylindrical beam of fragments. The optimisation of the design ensures that approximately equal numbers of fragments are propelled in all directions, i.e. there is a uniform distribution. Where the beam of fragments intersects with the aircraft structure, this can form a roughly regular and uniform distribution of fragmentation holes per unit area. This is a commonly accepted assumption supported by live-fire test results[5,6].

In order to model such widespread damage and to generate 'uniform' effects over an entire wing, the following method of simulating damage from multiple fragments was developed that could be applied over the entire surface of a wind tunnel model. As there are no results of prior testing available for simulated damage from multiple fragments, it is believed that this method defines a set of 'baseline' modelling characteristics for any future studies.

The number of fragment holes per unit area, within the region of damage is commonly defined as the 'fragment density', ρ_f. Fragment density was identified as a potentially key variable in this study. With reference to current Military Standards[6] a range of fragment densities was chosen to

https://doi.org/10.1017/S0001924000008472 Published online by Cambridge University Press

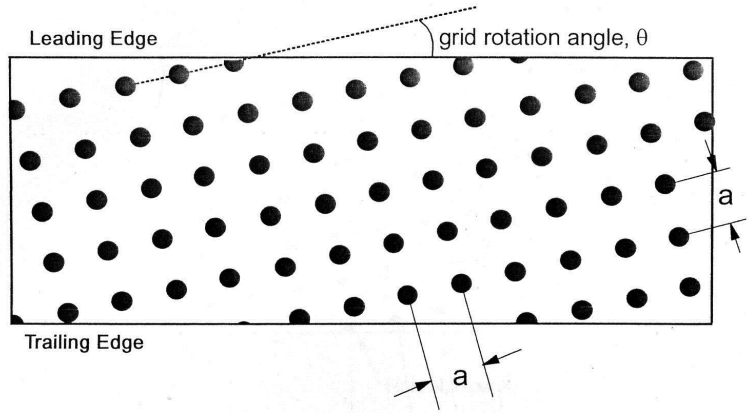

Figure 1. Grid of damage due to multiple fragment impacts.

reflect potentially survivable damage cases. These were ρ_f values of 10, 20 and 40 fragments per m^2. However, these were full-scale damage values applicable to actual aircraft. To apply the equivalent number of holes to the wind tunnel test wing a scaling factor was required, relating the model chord size (200mm) to a full-size wing chord. It was decided that a full-size mean chord value of 2m would be assumed. From this it was then possible to determine a value of the grid spacing; a for the wind tunnel model. This value defines the distance between damage centres (see Fig. 1) in both the chord and spanwise directions, and was determined by;

$$a = \frac{\text{model chord}}{\text{full size chord}} \sqrt{\frac{1}{\rho_f}} \qquad \ldots (1)$$

Given the assumption from live fire tests[5,6] of a regular uniform hole grid pattern, the placing of the grid on the wing planform had to be defined. The location of the holes relative to each other and to the oncoming flow required careful consideration. The orientation of the grid could have been between 0° and 360° relative to the leading edge. However, when at 0° or multiples of 45° orientation, holes downstream would sit directly in the wakes of those upstream. It was felt desirable, that the holes should be arranged such that their centres were distributed uniformly upstream of the trailing edge, with the minimum number of holes placed directly downstream of others. This would then give equally spaced wake centrelines along the trailing edge. This was achieved by a small rotation of the grid relative to the leading edge by an angle θ. The value of θ was calculated from the value of hole density ρ_f, the grid spacing value and the wing chord length.

Assuming a row had the centre of its first hole at the leading edge, then the maximum number of holes possible occurred along that row. The grid rotation angle was required to place the first hole in this row (Fig. 2, row *X*+l) directly upstream of the last hole in the preceding row (hole *N*, row *X*). In this way, all other rows (having less than or equal to the maximum number of holes possible) had their centres distributed uniformly upstream of the trailing edge. Given these methods for calculating hole spacing, a, and grid rotation angle, θ, each full-scale fragment density resulted in the model wing values shown in Table 1.

https://doi.org/10.1017/S0001924000008472 Published online by Cambridge University Press

Table 1
Damage hole grids

ρ_f	a	θ
10/m^2	31·6mm	9·5°
20/m^2	22·4mm	6·3°
40/m^2	15·8mm	4·7°

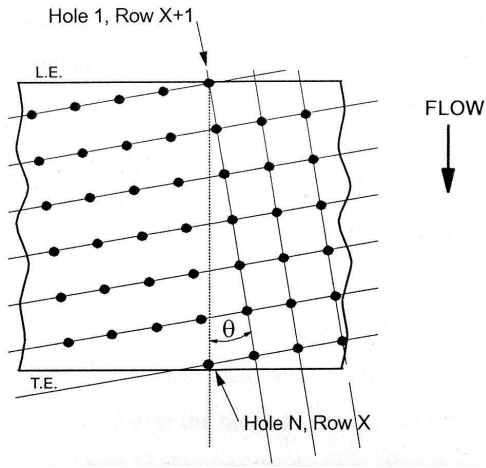

Figure 2. Grid hole alignment.

Missile fragment velocities can be up to approximately 2,000ms^{-1}. Given the relatively light weight construction of aircraft wings, live-fire tests have shown that fragments may pass straight through wing structures resulting in 'through-hole' damage. Through-hole damage was chosen to simulate missile fragment damage here, not only to reflect the above characteristics but also to remain consistent with simulated gunfire damage tests carried out in Ref. 1. As with gunfire damage studied in reference 1, the direction of penetration of the fragments was modelled as normal to the plan-view plane of the wing, i.e. at 90° to both chordline and leading edge. This resulted in the upper surface holes being located directly above those in the lower surface.

Experimental investigations[7,8] have shown that in tests designed to reproduce the effects of missile fragment impacts on aircraft structures, the damage could be approximated as being typically circular in shape, of a size similar to that of the missile fragment, and with negligible petalling around the edges. These characteristics were also found to vary little with fragment velocity in tests conducted over the range 541ms^{-1} to 1,666ms^{-1}. Consequently, circular shaped holes were used to simulate the damage due to the multiple warhead fragments. Hole diameters were defined in terms of fractions of the wing chord, and discussions with vulnerability specialists, suggested that damage hole diameters of 2·5%, 4%, 6% and 8% of wing chord, c, were typical for a 2m full-size wing chord. In the following text, these holes are denoted 2·5%c, 4%c, 6%c and 8%c.

Table 2 summarises the test cases investigated. Note that it was not physically possible to model 8%c damage at a fragment density equivalent to 40/m^2 (i.e. damage holes with diameters of 8%c, located 7·9%c between centres.)

https://doi.org/10.1017/S0001924000008472 Published online by Cambridge University Press

Table 2
Simulated fragment damage characteristics

ρ_f	Fragment damage hole diameters (%c)			
10/m^2	2·5	4	6	8
20/m^2	2·5	4	6	8
40/m^2	2·5	4	6	

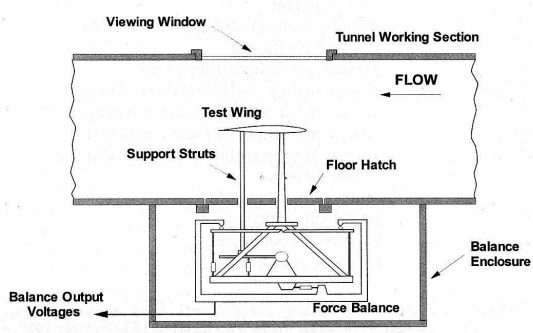

Figure 3. Wind-tunnel arrangement.

3.0 EXPERIMENTAL PROGRAMME

The test facility used to conduct the experimental studies was a 0·45m x 0·45m open-return low turbulence wind tunnel. This tunnel has a nominal turbulence level of 0·1%. A NACA 64_1-412 was chosen as a typical aircraft aerofoil section. This aerofoil was also used in previous investigations into gunfire damage. Full-span models, with natural transition were mounted, via struts, to a three-component wind tunnel balance (Fig. 3). The balance had a nominal accuracy of 0·05% full-scale deflection on each component. Data was recorded by a standard PC, via a dedicated data acquisition system, giving repeatability of C_l to within 0·015, C_d to 0·0005, and C_m to 0·001. Balance measurements were supplemented by smoke and titanium dioxide surface flow visualisation.

The tunnel corrections were based on blockage and wall-constraint correction factors for fully closed working-section tunnels recommended by AGARD[9]. However, AGARD recommends a maximum ratio of model chord to tunnel height for valid corrections. In the current experiments, this ratio was exceeded to allow the use of larger models, which facilitated more precise damage modelling. Accordingly, initial tests were carried out using two different chord sizes of the same (undamaged) aerofoil section, one below and one above the maximum ratio recommended. The results suggested that the standard correction procedure remained valid for the larger 200mm chord aerofoils used here. It should be noted that the wind-tunnel corrections were for an undamaged model, because there was no straight forward way of adapting the AGARD method for damage. Results from Irwin[1] for simulated gunfire damage were obtained using the same wind-tunnel arrangement and correction method. Use of Irwin's data to predict the effects of damage on finite aspect ratio wings tested in a significantly larger wind tunnel, and at lower blockage levels, produced satisfactory predictions away from the stall[3]. Based on this experience, it was concluded that errors introduced by basing the wind tunnel corrections on an undamaged model were likely to be acceptable.

https://doi.org/10.1017/S0001924000008472 Published online by Cambridge University Press

For the large number of damage cases considered in the complete research programme, it was necessary to develop a method of accurate model manufacture that was suitable for producing a large number of wings. A method using moulded glass-fibre reinforced composite construction was developed. All models were hollow and incorporated some degree of internal construction modelling, with the inclusion of leading and trailing edge spars centred at 20% and 65% chord locations. These spars were approximately 1%*c* in thickness, and were included to represent the typical 'three-box' cavity structure of an aircraft wing.

The simulated damage covered the entire surface of the model. To avoid intersection of damage holes with the strut mounting points, a small number of damage holes had to be omitted.

4.0 DAMAGE EFFECTS ON AERODYNAMIC COEFFICIENTS

Before applying any damage, the results for the undamaged aerofoils were compared with previously published data, Loftin and Smith[10]. The published data was at a Reynolds number of 7 x 10^5 compared with 5 x 10^5 for the present study. Although there was a slight mismatch in the Reynolds numbers, the differences between the two sets of data were entirely consistent with typical Reynolds number effects (e.g. higher C_d at lower Reynolds number).

For ease of comparison, the results for the damaged model are presented as changes in coefficients from the undamaged wing, where:

$$dC_l = C_{l\,damaged} - C_{l\,undamaged} \quad \ldots (2)$$

$$dC_d = C_{d\,damaged} - C_{d\,undamaged} \quad \ldots (3)$$

$$dC_m = C_{m\,damaged} - C_{m\,undamaged} \quad \ldots (4)$$

4.1 Changes in lift coefficient

The changes in lift coefficient for the different damage cases is summarised by Fig. 4, which plots dC_l values against incidence. It can be seen from this figure that all the test cases resulted in similar trends although to differing magnitudes. The results show that the least significant effect on lift resulted from the smallest damage size at the lowest fragment density (2·5%c at 10/m^2), and the greatest effect from the largest damage size at the highest density (6%*c* at 40/m^2). For the undamaged wing the zero lift angle was at approximately –3 degrees. For the damaged wings at higher incidences the pressure differential between the upper and lower surfaces resulted in a flow through the damage holes from the lower to the upper surface, resulting in a lift loss. At incidences significantly less than –3 degrees the through flow was reversed and relative to the undamaged wing there was an increase in the lift coefficient. At around –3 degrees a small lift loss occurred. Given the minimal pressure differential between the upper and lower surfaces close to this incidence, the flow through the damage holes was likely to be negligible. The lift loss was due to the area removed by the damage and by cavity type flows in the damage holes.

Figure 4 also indicates that some damage cases resulted in similar lift losses. For example, considering 6%*c* at 10/m^2, 4%c at 20/m^2 and 2·5%c at 40/m^2, at 8° of incidence these cases all resulted in dC_l values of –0·4570 ± 0·0035. These cases were found to have similar area losses (percentage of undamaged wing area removed) of 10·5%, 9·6% and 8·1% respectively. By plotting the values of dC_l against percentage wing areas lost for a given incidence, a relationship was seen across the range

https://doi.org/10.1017/S0001924000008472 Published online by Cambridge University Press

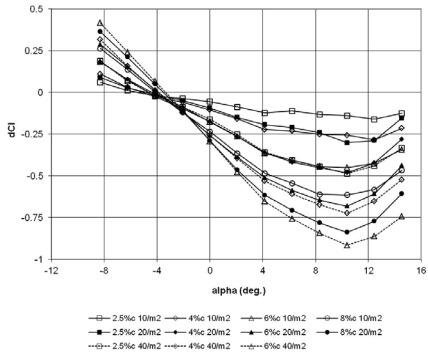

Figure 4. Lift coefficient increment *vs* incidence.

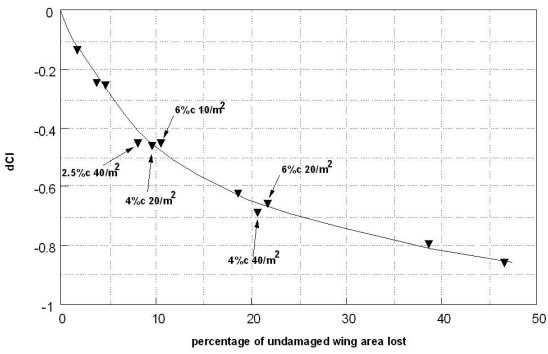

Figure 5. Lift coefficient increment *vs* wing area lost. 8° incidence.

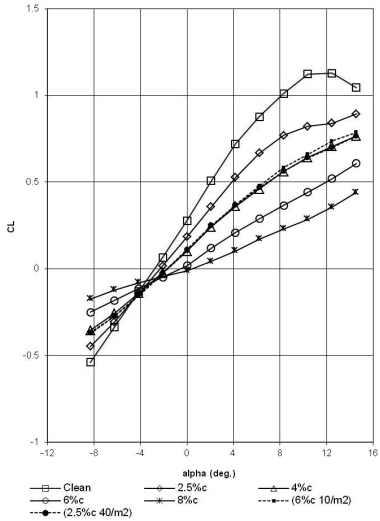

Figure 6. Lift coefficient *vs* incidence. (Results for ρ_f = 20/m² unless stated otherwise.)

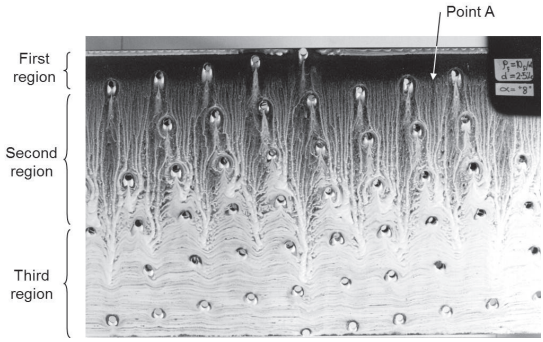

Figure 7. Upper surface flow visualisation. 2·5%c damage at ρ_f = 10/m². 8° incidence.

of test cases considered. Figure 5 illustrates the 8° results, which show that the lift loss increases as more wing area was removed, although the relationship is not directly proportional since doubling the area lost does not double the value of dC_l. Compared with the undamaged wing, all cases of multiple fragment damage produced reduced lift curve slopes up to the maximum incidence tested (+14°) and showed evidence of delayed stall. Figure 6 is included here to illustrate the characteristics seen. Lift curve slopes for the damage cases were seen to depend on the amounts of wing area removed. As with individual dC_l values, to a close approximation, the removal of similar percentages of area resulted in similar lift curve slopes for different combinations of ρ_f and damage size. This is illustrated by the results for 6%*c* at 10/m², 4%*c* at 20/m² and 2·5%*c* at 40/m² in Fig. 6.

Flow visualisation for the lowest level of simulated damage considered (2·5%*c* at ρ_f =10/m²) showed three distinct regions on the surface of the wing. The first was located between the leading edge and the first row of holes, where the surface flow appeared relatively unaffected by the presence of the holes. Figure 7 illustrates this at an incidence of +8°. For this figure, and all subsequent flow

https://doi.org/10.1017/S0001924000008472 Published online by Cambridge University Press

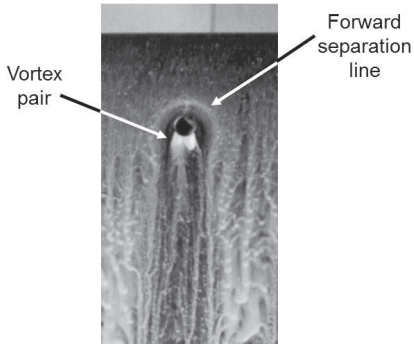

Figure 8. Enlargement of flow visualisation for single hole. 2·5%c damage at ρ_f = 10/m^2. 2° incidence.

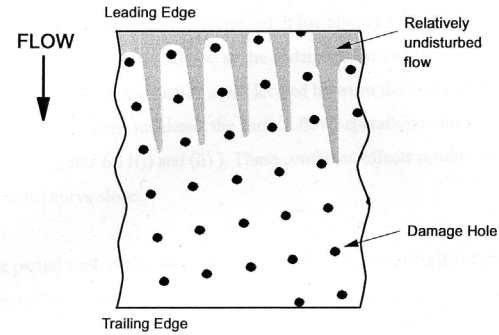

Figure 9. Sketch of regions of undisturbed flow.

visualisation pictures, the wing leading edge is at the upper edge of the picture and the flow is from top to bottom. At this incidence the undamaged wing had a laminar separation bubble located at the leading edge, and this can still be seen in Fig. 7 (except where intersected by two holes). The bubble was a characteristic of the undamaged aerofoil at low Reynolds numbers and was not caused by the damage. The second region started at the location of the first row of holes. Within this region, the clearest effects were seen for those holes on the first row. From detailed examination (Fig. 8) it was seen that the flow mechanisms present were very similar to those reported by Irwin and Render[1] for gunfire damage, but on a smaller scale. For each hole a forward separation line can be identified, where oncoming surface flow separated as a result of flow emerging through the hole. The collection of flow visualisation mixture at the hole rear edges, also indicated the presence of contra-rotating vortex pairs, as also seen for the larger gunfire damage. The majority of second region holes appeared to have characteristics similar to the 'weak-jets' previously observed for gunfire damage; i.e. the damage wake was attached to the surface with little spanwise increase in the wake width. Importantly, flow visualisation indicated no interaction between the flows of each hole. Indeed the majority of the surface flow, located in the gaps between the holes, appeared relatively unaffected by the wakes, and exhibited attached flow (Fig. 7 — point A). Progressing rearwards beyond the first few rows, it was seen that the accumulating attached wakes from the damage resulted in a progressive reduction in the spanwise width of the unaffected gap areas. It is suggested that areas of 'suction' were able to develop in the first and second regions, see Fig. 9. These areas would be what remained of the 'two-dimensional' pressure peak generated by an undamaged wing. In addition, Irwin and Render[1] showed that weak-jets produced relatively small changes in static pressure in the local flow field either side of damage. Therefore the suction areas developed as a result of the relatively undisturbed flow in the gap areas between the holes.

The flow visualisation indicated that the combined wakes in the second region separated from the surface to form a third region. As seen in Fig. 7, the forward edge of this region was ambiguous, but was seen to move forward with increasing incidence (approx 90%c, 60%c and 40%c locations for +2°, +8° and +12° respectively, for this damage case). Within this region, flow visualisation indicated only a small amount of through flow, as little titanium-dioxide collected at the hole edges. In fact, within the entire third region, the surface flow appeared very sluggish with little if any movement (Note the lack of disturbance in the spanwise 'bands', produced when applying the paint).

https://doi.org/10.1017/S0001924000008472 Published online by Cambridge University Press

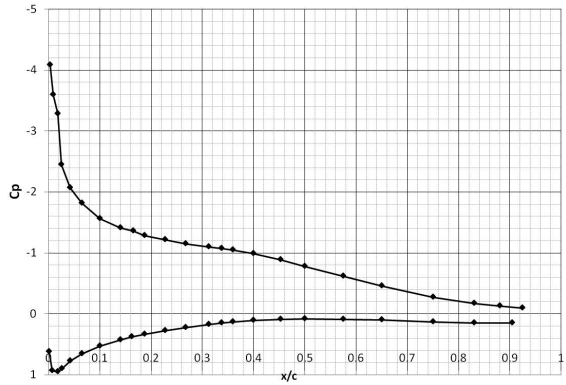

Figure 10. Pressure distribution for the undamaged wing. 8° incidence.

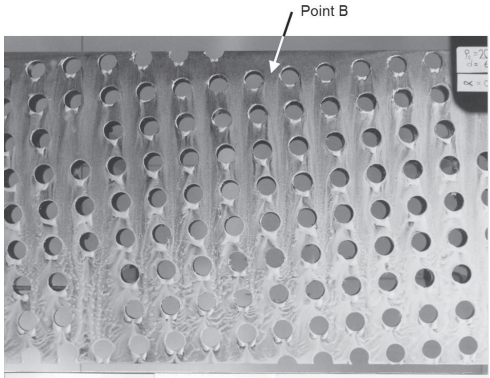

Figure 11. Upper surface. Flow visualisation. 6%*c* damage at ρ_f = 20/m^2. 0° incidence.

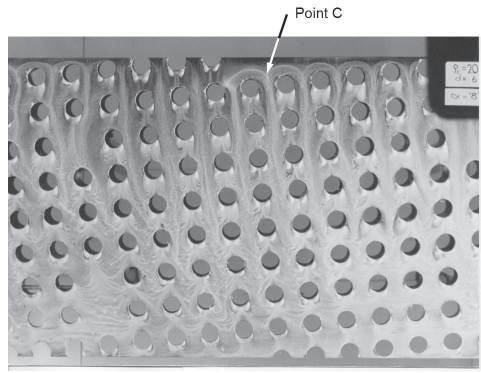

Figure 12. Upper surface. Flow visualisation. 6%*c* damage at ρ_f = 20/m^2. 8° incidence.

Static pressure measurements for the undamaged wing at a Reynolds number of 5 x 10^5 have been published by Irwin and Render[1] and the distribution at +8° is shown in Fig. 10. The first region identified in Fig. 7 extends to approximately 12% of wing chord which includes the suction peak and represents an area of significant pressure differences across damage holes in this region. The flows through the damage resulting from these pressure differences were seen as the previously identified weak jets in Fig. 7. From Fig. 10 it can be seen that the pressure difference between the upper and lower surfaces reduced as *x*/*c* increased. Consequently the flow through damage holes would also be expected to reduce with increasing *x*/*c*, and explains the absence of significant through flow seen in the third region.

The effects of increasing hole size and fragment density on the flow characteristics are illustrated in Figs 11 and 12 for 6%*c* at ρ_f = 20/m^2. Flow visualisation indicated that at low incidences, flow through the holes was limited. For the first few rows, the combination of boundary-layer growth and cumulative wake development, previously identified as the first and second regions, was again observed (e.g.: Point B, Fig. 11).

With increasing incidence, the amount of damage through flow increased, which in turn increased the size of the separation around the individual holes. Also, due to increases in ρ_f and/or damage diameter, the ratio of 'inter-hole gap to damage hole radii' decreased. Together, this resulted in the joining together of the separation regions around each hole in the forward-most row of holes

https://doi.org/10.1017/S0001924000008472 Published online by Cambridge University Press

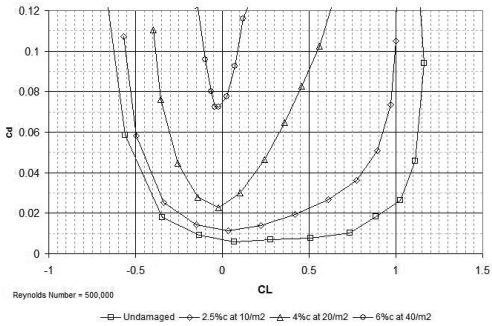

Figure 13. Drag coefficient *vs* lift coefficient.

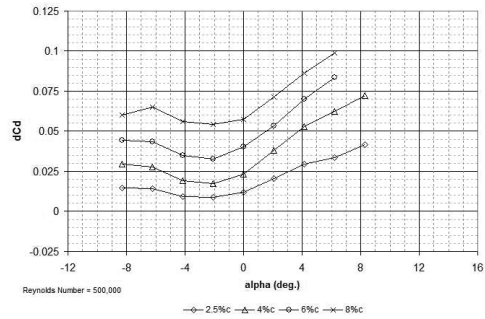

Figure 14. Drag coefficient increment *vs* incidence. $\rho_f = 20/m^2$.

(See point C, Fig. 12). Not only did the separation inhibit any development of a suction peak, but also 'forced' the upper surface flow to separate at the first row (across the span of the wing). Over the remainder of the chord the previously observed third region of sluggish surface flow was not seen. Instead, the increased through flow produced surface flow in a chordwise direction, over the remaining surface. This flow would have been comprised of the combined wakes of the upstream holes, which remained attached to the upper surface. Unfortunately, surface pressure data were not available for the damage due to multiple fragments cases, and it has not been possible to identify the details of the flow-field mechanics. However, it can be said that the effects are to delay a 'full' stall beyond +14°, and to continue to generate a reduced level of lift.

4.2 Changes in drag coefficient

In all of the damage cases, C_d increased significantly over the entire incidence range tested. This resulted from both the large numbers of surface discontinuities (i.e. holes) and the formation of the extensive regions of surface flow separation. Figure 13 illustrates the range of C_d values seen, with both the least and most severe damage cases tested. Compared with the undamaged wing minimum C_d of 0·0056, the least severe case (2·5%*c* at 10/m^2) resulted in a minimum C_d of 0·0113, a 102% increase. Whilst the worst case (6%*c* at 40/m^2) resulted in a corresponding value of 0·0724, a 1,190% increase. Also, the damage reduced the range of C_l between the drag rises.

Figure 14 indicates the drag increments dC_d *vs* incidence for the $\rho_f = 20/m^2$ damage cases tested. Firstly, it was seen that for a fixed ρ_f, dC_d values increased with hole size. Secondly, either side of the minimum dC_d values, dC_d increased with changing incidence and exhibited the same trends for each case. Indeed, similar shaped curves were seen for each hole size, with each effectively translated up the dC_d axis by different amounts.

For a constant hole size, dC_d increments with incidence could be explained by increased through flow resulting in greater separation on the exit surface. With holes in the range 4%c to 8%*c* ($\rho_f = 20/m^2$) showing similar surface flow separation from the forward most row of holes (as discussed previously), it was not surprising that Fig. 14 exhibited similar dC_d gradients for these cases. This was seen to be true for similar forward separations at different ρ_f values. However, when some degree of undisturbed surface flow between the holes had been observed (as seen in Fig. 7 for 2·5%c at $\rho_f = 20/m^2$), a reduced dC_d gradient resulted above 0°.

In all cases the minimum drag coefficient increment occurred at –2°. This is close to the zero lift angle where the least average through flow would be expected (based on undamaged C_p values

https://doi.org/10.1017/S0001924000008472 Published online by Cambridge University Press

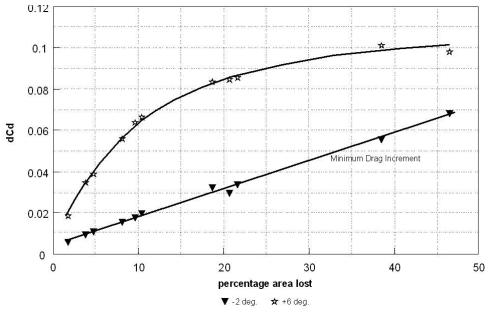

Figure 15. Drag coefficient increment *vs* wing area lost.

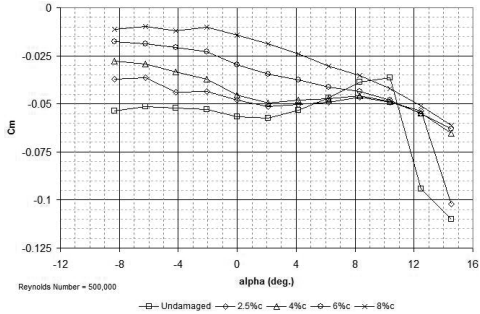

Figure 16. Pitching moment coefficient *vs* incidence. ρ_f = 20/m^2.

reported by Irwin and Render[1]. Hence damage induced separation would be minimal. Plotting the minimum drag coefficient increment, it was found that for all cases tested, the values had an approximately linear relationship with percentage wing area lost (Fig. 15). Varying incidence, it was found that dC_d remained related to the total wing area removed by the damage, although the nature of the relationship varied with incidence (Fig. 15).

4.3 Changes in pitching moment coefficient

Figure 16 shows the C_m results for the ρ_f = 20/m^2 damage tests. The differences observed between the undamaged and damaged cases result from the combined effects of removed wing area, upper surface flow separation and suction area development. It was found that a clear trend existed, in that the larger the damage size (for a given ρ_f) the larger the effect on C_m values. For low incidences, both 2·5%*c* and 4%*c* results gave similar C_m profiles, which were in themselves not too dissimilar to the undamaged wing, whilst 6%c and 8%c results showed greater differences. Adding damage delayed the abrupt change in C_m seen for the undamaged wing at around 10° incidence. As discussed for Fig. 6, this was due to the damage delaying the stall to higher incidences. Interestingly, it was found that moving to higher positive incidences, 4%*c*, 6%*c* and 8%*c* results tended towards similar values. This may be attributable to the separation of the upper surface flow from the forward-most row of holes for these cases. It was found that similar variations with damage size were exhibited at all ρ_f values tested, with the largest diameter holes at the highest ρ_f giving the closest results to zero C_m. Without the aid of surface pressure data for the multiple fragment damage cases, this effect is difficult to explain, and in general it is not possible to comment further on these C_m results.

5.0 INFLUENCE OF WING CONSTRUCTION ON AERODYNAMIC CHARACTERISTICS

For gunfire damage, internal construction of the wing has been shown to influence the measured lift, drag and pitching moment increments[11]. Similarly the consequences of different internal wing construction were considered for damage due to multiple missile fragments by also testing a solid model of the NACA 64$_1$-412. Typical results are illustrated by Figs 17 to 19, which are for 4%*c* at ρ_f =20/m^2.In general, it was found that the effects of damage on the solid wing coefficients followed very similar trends to those seen for the hollow wing, although the magnitudes of the effects were found to differ. Figure 17 illustrates that the solid wing had both the greatest rate of

https://doi.org/10.1017/S0001924000008472 Published online by Cambridge University Press

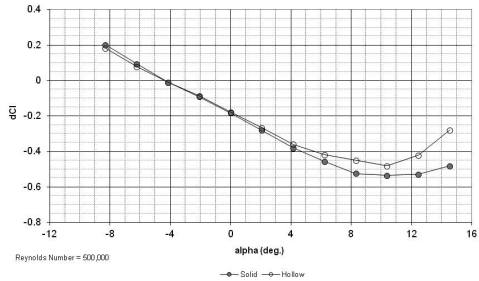

Figure 17. Comparison of lift coefficient increment *vs* incidence for solid and hollow models. 4%*c* damage at ρ_f = 20/m^2.

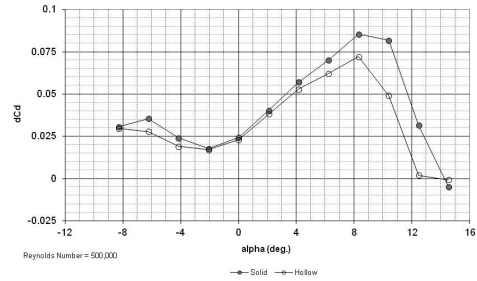

Figure 18. Comparison of drag coefficient increment *vs* incidence for solid and hollow models. 4%*c* damage at ρ_f = 20/m^2.

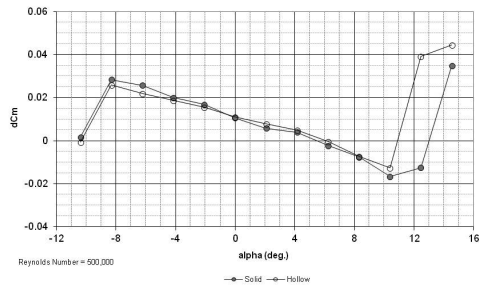

Figure 19. Comparison of pitching moment coefficient increment *vs* incidence for solid and hollow models. 4%*c* damage at ρ_f = 20/m^2.

dC_l change with incidence, and the greatest positive and negative dC_l values (an 11·2% increase from –0·4813 to –0·5352, at +10° incidence). The differences between solid and hollow aerofoil dC_d values were seen to increase with incidence (Fig. 18). This may have been as a result of solid wing through flow influencing the development of the upper surface separation region. Possible increases in exit flow from holes near the leading edge may have resulted in an increased propensity for separation, and thus increased dC_d values. The exit flow increase may have resulted from the inability of the through flow to circulate internally within the wing and exit from a hole further 'downstream' than the entry hole.

C_m measurements for both solid and hollow wings indicated similar effects, with solid construction again giving slightly greater dC_m changes. Similar effects were again seen for damage of differing hole sizes.

6.0 APPLICABILITY OF RESULTS

Manned aircraft and many uninhabited aerial vehicles (UAVs) operate at Reynolds numbers in excess of 5 x 10^5 which has been considered in this study. Based on the authors' experience of testing simulated gunfire damage over a range of Reynolds numbers with both forced and natural transition[2], it is believed that the trends and magnitudes of coefficient increments reported here will be replicated at higher Reynolds numbers. Similarly many of the reported flow features introduced by damage will be present at higher Reynolds numbers This is particularly true at incidences above approximately 4 degrees where the laminar separation bubble,

https://doi.org/10.1017/S0001924000008472 Published online by Cambridge University Press

and hence transition, was located close to the leading edge of the undamaged wing.

For some of the damage cases the resulting coefficient increments are relatively small. However, such increments may still be significant in terms of whether an aircraft can return to base or make a safe diversion. Increased drag resulting from damage will increase fuel burn and may limit the diversion options for an aircraft. Reductions in maximum lift coefficient will result in an increased stall speed and limit an aircraft's ability to manoeuvre, for example in turning finals on to a landing approach or in manoeuvring to avoid enemy fire. The size of increments reported here will be further magnified when they are in close proximity to leading edge and trailing edge controls. Render[2] has shown that the aerodynamic effects of single hole damage are increased with increasing wing camber, and this trend has been confirmed for a simple trailing edge flap attached to a two-dimensional NACA 0012 wing[12].

7.0 FURTHER WORK

This paper is believed to be the first published study into the aerodynamic effects of damage resulting from multiple missile warhead fragments. It represents an initial investigation and should form the basis of further studies. Two key areas for further investigation are:

- The influence of damage from multiple fragments on the aerodynamic characteristics of finite aspect ratio wings — Studies by Render[3] and Pickhaver[13] have shown that the aerodynamic effects of single hole damage on a three dimensional wing can be predicted using the pressure distribution of the undamaged three dimensional wing and the results from damage on a two dimensional wing. Whether a similar technique can be used for damage from multiple fragments needs to be investigated.
- The performance of leading edge and trailing edge controls in the presence of damage from multiple fragments — The presence of battle damage will reduce the effectiveness of conventional aircraft controls[12] and these effects need to be quantified in further investigations.

8.0 CONCLUSIONS

- In all of the cases tested, simulated damage from multiple missile warhead fragments resulted in significant C_l losses, C_d increases and C_m changes. Increasing fragment density or hole diameter made the effects greater. All damage cases delayed full stall to beyond the maximum incidence tested.
- Two different damage cases which remove the same area from the wing will produce similar values of the drag and lift coefficient increments. Increasing the amount of wing area removed will increase the size of the lift and drag increments. However, the relationship between increments and area removed was shown to be non-linear.
- Low fragment densities and smaller damage sizes resulted in a complex surface flow structure made up of boundary layer growth between the damage holes, attached damaged wakes from the forward holes and detached surface flow from the rear holes. Individual hole patterns were similar to those reported for larger scale gunfire damage cases.
- Increased fragment density and hole size resulted in the upper surface flow separating at the first row of holes. Behind this separation, the flow was attached and consisted of the combined wakes of the forward damage holes.

https://doi.org/10.1017/S0001924000008472 Published online by Cambridge University Press

- Investigations into the influence of internal model construction indicated that trends in coefficient increments were similar for both hollow and solid wings. However, the magnitudes of the effects were found to be smaller for hollow wings than for solid wings. This indicates that for accurate damage modelling, wind tunnel models must reflect the true nature of the full scale wing construction.

REFERENCES

1. IRWIN, A.J. and RENDER, P.M. Influence of mid-chord battle damage on aerodynamic characteristics of two-dimensional wings, *Aeronaut J*, March 2000, **104**, (1033), pp 153-161.
2. RENDER, P.M., DE SILVA, S, WALTON, A.J. and MAHMOUD, M. Experimental investigation into the aerodynamics of battle damaged airfoils, *J Aircr*, 2007, **44**, (2), pp 539-549.
3. RENDER, P.M., SAMAD-SUHAEB, M., YANG, Z. and MANI, M. Aerodynamics of battle damaged finite-aspect-ratio wings, *J Aircr*, June 2009, **46**, (3), pp 997-1004.
4. SAEEDI, M., AJALLI, F. and MANI, M. A Comprehensive numerical study of battle damage and repairs upon the aerodynamic characteristics of an aerofoil, *Aeronaut J, 2010,* **114**, pp 469-484.
5. Survivability aircraft non-nuclear, General criteria, 1982, MIL-HDBK-336-1, Vol 1.
6. UK Defence Standard 00-970 Part 13 Design and airworthiness requirements for service aircraft, Section 3, 2011.
7. Addendum to design manual for impact damage tolerant aircraft structure, 1988, AGARD-AG-238 (Addendum).
8. KAGERBAUER, G. *ET AL*. Improvement of battle damage tolerance for composite structures, 1986, AGARD Report 729 — Impact Damage to Composite Structures.
9. GARNER, H.C. ET AL. Subsonic wind tunnel wall corrections, *AGARDograph*, October 1986, **109**.
10. LOFTIN, L.K. and SMITH, H.A. Aerodynamic characteristics of 15 NACA airfoil sections at seven Reynolds numbers from 0·7 x 10^6 to 9·0 x 10^6, 1945, Technical Note, National Advisory Committee for Aeronautics.
11. IRWIN, A.J and RENDER, P.M. The influence of internal structure on the aerodynamic characteristics of battle damaged wings, 1996, Paper 96-2395, 14th AIAA Applied Aerodynamics Conference.
12. RENDER, P.M and WALTON, A. Aerodynamics of battle damaged wings — The influence of flaps camber and repair schemes, 2005, Paper 2005-4721, 23rd AIAA Applied Aerodynamics Conference.
13. PICKHAVER, T. and RENDER, P.M. A technique to predict the aerodynamic losses of battle damaged wings, 2012, Paper ICAS 2012-3.2.2, 28th International Congress of the Aeronautical Sciences.

https://doi.org/10.1017/S0001924000008472 Published online by Cambridge University Press